

Electron drift directions in strong-field double ionization of atoms

To cite this article: S L Haan *et al* 2009 *J. Phys. B: At. Mol. Opt. Phys.* **42** 134009

View the [article online](#) for updates and enhancements.

Related content

- [Fast Track Communication](#)
S L Haan, Z S Smith, K N Shomsky *et al.*
- [Universal time delay in the recollision impact ionization pathway of strong-field nonsequential double ionization](#)
Qiangang Li, Yueming Zhou and Peixiang Lu
- [Laser-assisted collision effect on non-sequential double ionization of helium in a few-cycle laser pulse](#)
Hongyun Li, J Chen, Hongbing Jiang *et al.*

Recent citations

- [Correlated electron dynamics in strong-field nonsequential double ionization of Mg](#)
Ning Li *et al*
- [Recollision dynamics in nonsequential double ionization of atoms by long-wavelength pulses](#)
Cheng Huang *et al*
- [Electron dynamics of molecular double ionization by elliptically polarized few-cycle laser pulses](#)
Tong Ai-Hong *et al*

Electron drift directions in strong-field double ionization of atoms

S L Haan, Z S Smith, K N Shomsky and P W Plantinga

Department of Physics and Astronomy, Calvin College, Grand Rapids, MI 49546, USA

E-mail: haan@calvin.edu

Received 30 December 2008, in final form 15 March 2009

Published 12 June 2009

Online at stacks.iop.org/JPhysB/42/134009

Abstract

Longitudinal momentum spectra and electron drift directions are considered for several laser wavelengths in non-sequential double ionization of helium using three-dimensional classical ensembles. In this model, the familiar doublet for wavelength 800 nm and intensities of order $5 \times 10^{14} \text{ W cm}^{-2}$ becomes a triplet for wavelength 1314 nm, then a doublet for 2017 nm. The results are explained based on whether the post-ionization impulse from the laser results in backward drift for one or both electrons.

(Some figures in this article are in colour only in the electronic version)

1. Introduction

A signature of non-sequential double ionization (NSDI) of atoms by intense laser fields [1] is a two-hump structure [2] in the electron net or sum momentum, when measured parallel to the laser polarization axis¹. The double hump is evidence that electron pairs are likely to drift out on the same side of the nucleus [3, 4]. This behaviour is in contrast to what occurs in sequential ionization, where the electrons ionize independently and are as likely to emerge on opposite sides of the nucleus as on the same side. In sequential ionization, cancellation in the sum momentum leads to a single peak centred at zero [5].

Much of the NSDI process, including the production of correlated electron pairs, can be described using classical or semiclassical physics because of the strength of the laser field and the continuum or quasi-continuum nature of the relevant quantum states. In the original recollision [6] model, one electron ionizes (through tunnelling) and is pushed outward by the oscillating laser field, but is then propelled back to the core where recollision transfers energy to the other electron. One possibility—if there is sufficient energy—is recollision impact ionization. If effects of the nucleus are ignored, both electrons would then be travelling forward (relative to the recollision) immediately after the recollision. However, the laser can deliver a post-ionization impulse [7] that sends the two electrons into the backward direction [3, 8].

¹ For our conditions of interest, the net momentum spectrum is similar to the ion momentum, since the only external force on the system is the laser, and its net force is zero.

Details depend on laser phase and the electrons' speeds just after the collision, as we will discuss below.

The use of fully classical 3D ensembles for studying NSDI was introduced in [8]. In the ensemble, the doubly ionized electron pairs most often drift into the backward direction, at least for laser wavelengths in the vicinity of $\lambda = 780 \text{ nm}$ and intensities about $5 \times 10^{14} \text{ W cm}^{-2}$. For these laser parameters, the returning electron can have sufficient energy for recollision impact ionization, but [8] found that it was more common for the recollisions to result in one free electron and one excited—but nonetheless bound—electron. The free electron would typically be pushed into the backward direction by the laser field. The bound electron would be pulled back by the nucleus, and escape into the backward direction over a suppressed potential-energy barrier at the next laser maximum. Haan and Smith [9] dubbed the latter process the 'boomerang.'

The laser phase and electron velocity at escape influence the final direction of motion. If an electron escapes before the field maximum, then to first approximation, it can be expected to drift into its direction of escape. For an electron that has just been excited in recollision, this direction is backward relative to the recollision. Thus both recollision impact ionization and recollision excitation with the boomerang can lead to same-hemisphere electrons [10]. However, recollision-excited electrons that escape over the barrier too late in the laser cycle (to first approximation, after the field maximum) drift opposite from their initial escape, thus into the forward direction relative to the recollision and opposite from the other electron.

In some trajectories the excited electron does not escape during the first laser maximum after recollision. Thus,

recollision excitation with subsequent ionization (RESI) [11, 12] can lead to pulses of final ionization in either direction. It is also possible for a free electron to scatter off the nucleus just before or just after recollision. Such backscattering has been shown to be the source of electrons with energy above $2U_p$ in NSDI [9, 10, 13–16]. Here U_p denotes the ponderomotive energy, $E_0^2/(4\omega^2)$, where E_0 is the laser field amplitude and ω is the frequency. (We use atomic units unless specifically indicated otherwise.) $2U_p$ is the maximum drift energy for an electron that starts from rest in an oscillating electric field. At shorter wavelengths, such as 390 nm, high-energy electrons can also be produced through the boomerang [9].

In this work, we consider various laser wavelengths as in the experimental work of Alnaser *et al* [17] for argon and neon, thus changing U_p and the recollision energy without changing the laser intensity. This allows us to explore situations where recollision can lead to either backward and forward drifting electrons.

2. The classical ensemble method

We employ 3D fully classical ensembles as in [8–10, 18]. Ensemble size is typically 2 million². We use six random numbers and a chosen distribution function to assign x , y and z positions for each electron. For results we will show here, we used a Gaussian distribution. We then calculate the potential energy

$$V(\mathbf{r}_1, \mathbf{r}_2) = -\frac{2}{\sqrt{r_1^2 + a^2}} - \frac{2}{\sqrt{r_2^2 + a^2}} + \frac{1}{\sqrt{|\mathbf{r}_1 - \mathbf{r}_2|^2 + b^2}}. \quad (1)$$

In this equation a and b denote Coulomb softening parameters. We soften the nuclear potential with $a = 0.825$ to prevent autoionization, as we discuss below. The electron–electron softening parameter b is included primarily for numerical stability; we typically set $b = 0.05$.³ Next, we determine the available kinetic energy so that the system will have energy of the helium ground state, -2.9035 au. Any positions outside the classically allowed regions (which would give negative kinetic energy) are rejected. We divide the kinetic energy between the two electrons using a random number in momentum space. With our eighth and ninth random numbers we select a sign for the radial motion of each electron; we set transverse velocities to zero⁴. Each atom is allowed to propagate for a time equivalent to one laser cycle (about 100 au) before the laser pulse. During this time the electrons jostle each other, transferring energy and angular momentum. The resulting distributions are basically independent of our original radial distribution function. It is important, though, that the starting state be spherically symmetric because non-symmetric distributions do not relax into symmetric ones

² We use shell scripts to divide the ensemble among processors on multiple desktop computers. Each processor works sequentially through 50 000 trajectories, and writes the doubly ionizing trajectories to a file. These output files are then assembled into one master file.

³ Higher b values can decrease the DI yield because of weaker recollisions.

⁴ We find that if we allow for transverse motion, the DI yield decreases. We inferred that the resulting high angular momentum electrons were more difficult to ionize through recollision.

on the necessary timescale. There is no apparent subset of our initial phase space that leads to double ionization; instead, trajectories that doubly ionize can be found throughout phase space. Indeed, there is a chaotic element to individual trajectories that will need to be discussed elsewhere.

The softening of the Coulomb potential is necessary to prevent having one electron dive deep into the Coulomb well and transfer sufficient energy to the second electron for it to escape the atom. It is straightforward to show from equation (1) by considering the removal of one electron to infinity that a must be at least 0.69 au to prevent autoionization. There is an upper limit on a as well, in order to be able to place two repelling electrons into the shallower well and still achieve total energy -2.9035 . We find that we need $a < 0.894$. In this paper, as in previous ensemble work, we start each run with $a = 0.825$, which gives good DI yield. The nucleus remains fixed at the origin at all times.

We treat the laser as an oscillating laser field that is uniform in space: $E(t) = E_0 f(t) \sin(\omega t)$. The function $f(t)$ is trapezoidal, since then there is no net kick to the electron during laser turn on or turn off [19]. Each two-electron trajectory is found numerically by integrating Newton’s second law⁵. The first ionization occurs as a result of barrier suppression and e–e repulsion—there is no tunnelling in this model. The depth of the nuclear potential energy well for the remaining electron is $-2/0.825 = -2.42$. A range of energies is available to this electron. It is not left at rest at the bottom of the well.

The softening of the nuclear Coulomb potential when both electrons are bound can be seen as a necessary adaptation of the classical model to allow for the quantum ground state. By contrast, an unbound electron that scatters off a nucleus can experience a large deflection, indicating that it experiences an unscreened nuclear potential. In order to allow for the possibility of nuclear scattering at recollision, we have adjusted our model from that first presented in [8]. In particular, as soon as one electron is ten or more atomic units from the nucleus, we decrease the screening parameter for both electrons, as described in [9, 10]. To conserve energy when we change a , we give each electron an appropriate kinetic energy boost in its radial motion. This ‘toggle switch’ change in a is somewhat unsatisfying but appears necessary for a fully classical model. For processes we will discuss in the present work, only the long-range behaviour of the nuclear force is important, and we present only the case where the final value of a is 0.4.

Because our computer program writes the position and momentum coordinates at regular intervals, it is straightforward for us to examine each doubly ionizing trajectory every 0.01 cycles (more often at low laser frequencies) and identify the final ionization times for each electron. For definiteness, we define an electron to be ionized if it achieves, and then maintains for at least 0.2 cycles, any of $E > 0$, where E is its energy, inclusive of electron–nucleus and e–e interactions but not the laser interaction; $|z| > 10$; or

⁵ We use ‘black box’ subroutines with adjustable tolerances for successive intervals 0.001–0.01 laser cycle in length (depending on laser frequency), and record all position and momentum values between these intervals. We adjust the tolerances to ensure stability of our results.

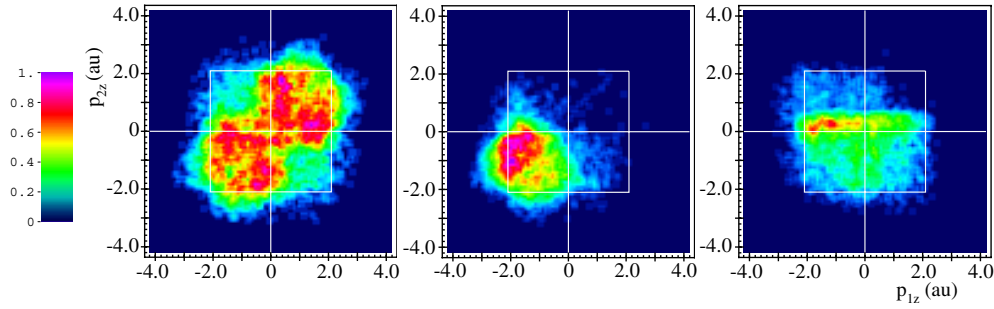


Figure 1. Final momentum along the laser polarization (z) axis for one DI electron versus the other for $\lambda = 800$ nm, $I = 0.5$ PW cm $^{-2}$ for a 10 cycle (2+6+2) pulse, with softening parameter $a = 0.4$. Left: no distinction between electrons. Centre and right: recolliding electron versus struck electron, with forward direction relative to recollision defined as positive. In the centre plot we include trajectories with time delay up to 0.25 cycles, on the right those with time delay above 0.25 cycles. Ensemble size is 2 million, giving 12 283 double ionizations. Scaling factor for the left plot is 82:1 and for the other two plots is 129:1 (i.e., the maximum number of counts in any bin is 82 for the left plot).

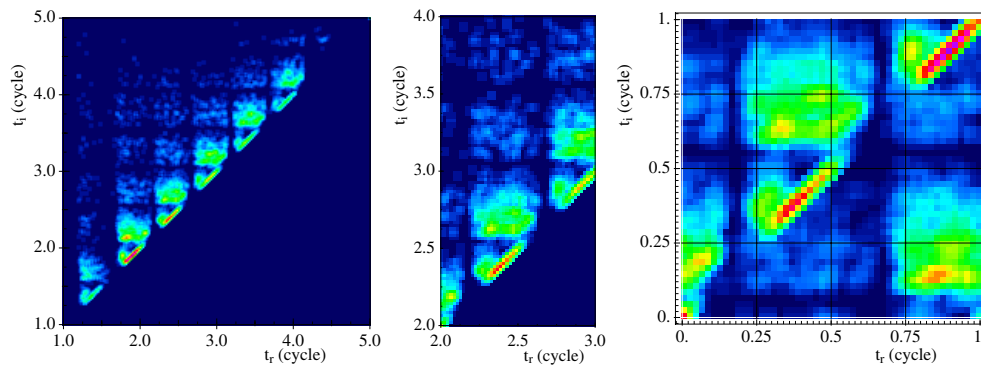


Figure 2. Time of final ionization versus time of recollision for all DI trajectories in a 5 cycle pulse for $\lambda = 800$ nm, $I = 0.5$ PW cm $^{-2}$, and $a = 0.4$. In the centre we zoom in 1 cycle. On the right we allow for wraparound to collapse all data to 1 cycle. Ensemble size is 2 million. The rightmost plot is scaled independently. Peak maxima occur at the quarter cycle ($n + 0.25$ and $n + 0.75$ c), zeros at the half cycle ($n, n = 0.5$ c). Recollision impact ionization occurs over a range of laser phases, indicated by population along the diagonal. Scaling factors for the left two plots are 137:1, and for the rightmost plot 254:1.

$zF_z > 0$ with $z^2 > 5$, where F_z is the longitudinal component of the net force. The final test basically checks whether the net force on the electron is towards or away from the nucleus, an indicator of whether particle is inside or outside the nuclear well. We then scan the time interval from when one electron first ionizes until final ionization of both electrons, and we call the time of closest approach the recollision time.

We test the stability of our results by adjusting ensemble sizes and ensuring convergence. All plots that we show in this paper are nearly identical to what would be obtained for ensembles of 1 million rather than 2, except for the number of outliers and an obvious factor of 2 in the number of counts.

3. Wavelength $\lambda = 800$ nm

We consider first wavelength $\lambda = 800$ nm and laser intensity 5×10^{14} W cm $^{-2}$ ($U_p = 1.10$). In figure 1 we show final longitudinal momentum of one DI electron versus the other. Pulse length is 10 cycles (2 cycles turn-on+6 cycles full strength+2 cycles turn-off). We also allow the system to propagate for one laser period after turnoff. The boxes show momentum $2\sqrt{U_p}$. On the left, we make no distinction between the electrons. Population extends beyond the box,

but the sum momentum $|p_{1z} + p_{2z}|$ has maximum value close to $4\sqrt{U_p}$. In the centre and right-hand plots we define the direction of recollision (the longitudinal direction of motion of the returning electron just before recollision) as positive, and we plot the final longitudinal momentum of the recolliding electron versus that of the struck electron. The centre plot includes trajectories with time delay, from recollision to final ionization, of up to 0.25 cycles. Most of the population lies in the third quadrant, indicating that both electrons drift into the backward direction relative to the recollision. The third plot considers trajectories that have time delay more than 0.25 cycles, and shows a more distributed population. The most conspicuous feature of the rightmost plot may be the band just above the p_{2z} axis. Here the recolliding electron drifts into the *forward* direction relative to the recollision, up to a certain cutoff momentum. Below, we interpret these in terms of recollision–excitation trajectories in which the free electron has sufficient energy after the collision to overcome the backward push from the laser and to drift into the forward direction.

In the leftmost plot of figure 2 we plot final ionization time versus recollision time for a 5 cycle (1+3+1) pulse. Impact DI is indicated by population along the diagonal. Because of

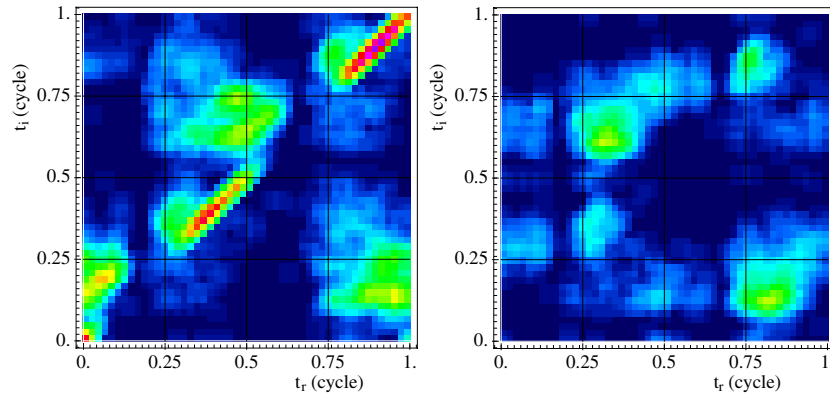


Figure 3. Similar to the rightmost plot of figure 2, but with trajectories separated based on whether the DI electron pairs drift out in the same (left plot) or opposite (right plot) longitudinal directions. Colour scale is the same for both plots, but independent from figure 2. We interpret the population clusters in the right plot near $(0.32, 0.65)$ and $(0.82, 0.15)$ as resulting from recollision excitation in which one electron has sufficient energy after recollision to drift out into the forward direction. Scaling factor is 245:1.

the 1 cycle laser turn on, recollisions do not begin until about $1.25 c$ and do not reach maximum energy until the interval from $1.75 c$ to $2 c$. Other DI populations can be associated with RESI. For each half pulse, considerable ionization is evident at the first laser maximum after recollision, with decreasing amounts at subsequent maxima. There are dark bands indicating times when recollisions or ionizations do *not* occur. It is significant how small these bands are. Recollisions are not simply clustered around the laser zeros, but occur over a significant range of laser phases.

Because of the difficulty in seeing details in the leftmost plot, we zoom in on recollision time from 2 to 3 c in the centre plot of figure 2. In the rightmost plot, we include all DI pairs and allow for wraparound, plotting laser phase at final ionization versus laser phase at recollision (denoted by t_i and t_r , respectively, and measured in laser cycles). The plots show that recollision impact ionization occurs in time intervals from just after peak field (0.25 and $0.75 c$) until the field zero (0.5 and $1.0 c$). There is a clear ‘shadow’ of slightly delayed ionization (around $(t_r, t_i) = (0.3, 0.4)$ and $(0.5, 0.9) c$) while the field is strong. Also clearly evident is DI from slowdown collisions, in which recollision occurs after the field zero so that the returning electron is travelling against the laser force. Such collisions were very important in 1d [20] where there was, in effect, only one impact parameter for the recollisions and it was important to match the motions of the returning and bound electrons so as to maximize energy transfer. In 3D, electrons return with a variety of impact parameters, and a wider range of recollision times is effective.

In figure 3 we divide the population of figure 2 into two parts, based on whether the electrons drift out with the same or opposite signs for final p_z . We shall occasionally refer to these two cases as emerging in the same or opposite hemispheres. The plot on the left is a reminder that recollision impact ionization leads primarily to same-hemisphere electrons. In addition, the considerable population off diagonal is a reminder of the importance of RESI. Haan *et al* [10] discussed how recollision excitation with final ionization at the next laser maximum can be an important source of correlated electron pairs, often with one electron pushed back by the

laser and the other boomeranging. In the right-hand plot, ionizations during time periods in which the laser field is waning (t_i from $0.25 c$ to $0.50 c$ and again $0.75 c$ to $1.00 c$) are a reminder that anticorrelated electrons can be produced if final escape occurs after the field maximum [8]. But the most noticeable characteristic of the right-hand plot may be the clusters near $(t_r, t_i) = (0.32, 0.65) c$ and $(0.82, 0.15) c$, which indicate oppositely directed electrons even though final emission occurs before the field maximum. These have time delay greater than $0.25 c$, and thus were included in the right plot of figure 1. Below, we will interpret these clusters in terms of the recollision-excitation trajectories in which the free electron has sufficient energy after the collision to drift into the forward direction.

We consider next the net or sum longitudinal momentum, $p_{1z} + p_{2z}$. On the left in figure 4 we show the net longitudinal momentum spectrum for increasing time delay between recollision and final ionization. As in figure 5 of [10], which considered $\lambda = 780$ nm and intensity $4 \times 10^{14} \text{ W cm}^{-2}$, a doublet forms for time delays of a portion of a laser cycle, then fills in. The left–right asymmetry arises based on which direction the electric force points first. The centre and right plots apply for wavelengths 1314 and 2017 nm, and will be discussed below.

4. Wavelength $\lambda = 1314$ nm

Changing the laser wavelength but maintaining the same laser intensity changes the ponderomotive energy U_p and thus the energy available at recollision. Elsewhere [18], we have considered the smaller wavelength $\lambda = 483$ nm. For that case, the net momentum spectrum was a singlet and the most common route to DI was recollision with a short-lived doubly excited state. In the present work we consider longer wavelengths, so that the recollision energy is increased. Pulse length remains 5 cycles.

Phase plots for same-hemisphere and opposite-hemisphere electrons for $\lambda = 1314$ nm ($U_p = 2.97$) are shown in figure 5. For these laser parameters, there

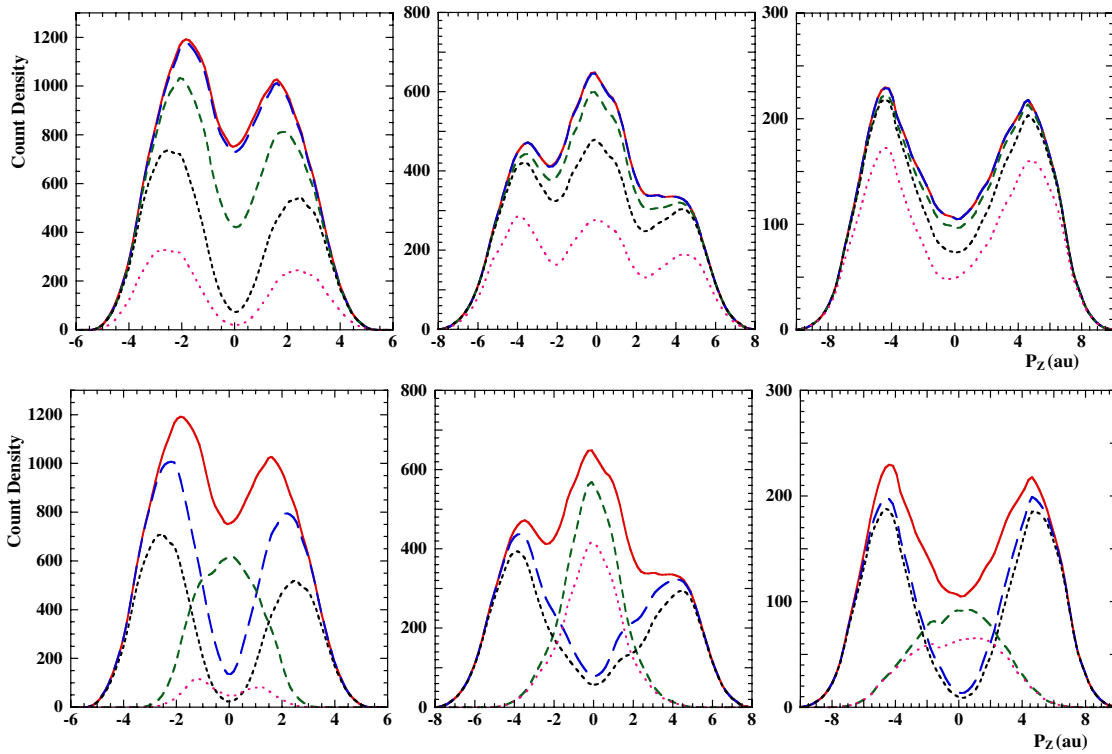


Figure 4. Spectrum of net longitudinal momentum for $I = 5 \times 10^{14} \text{ W cm}^{-2}$ and for $\lambda = 800 \text{ nm}$ (left), 1314 nm (centre), and 2017 nm (right) for 5 cycle pulses. Top row shows maximum time delays (recollision to final ionization), from bottom to top, 0.06 c , 0.26 c , 0.50 c and 2.00 c . Top curves show full spectra through the end of the pulse. The second row divides the populations by whether the electrons are in the same or opposite hemispheres (outer and inner peaks, respectively). Lowest curves show time delay less than 0.25 c and the middle curves the full pulse for the different categories.

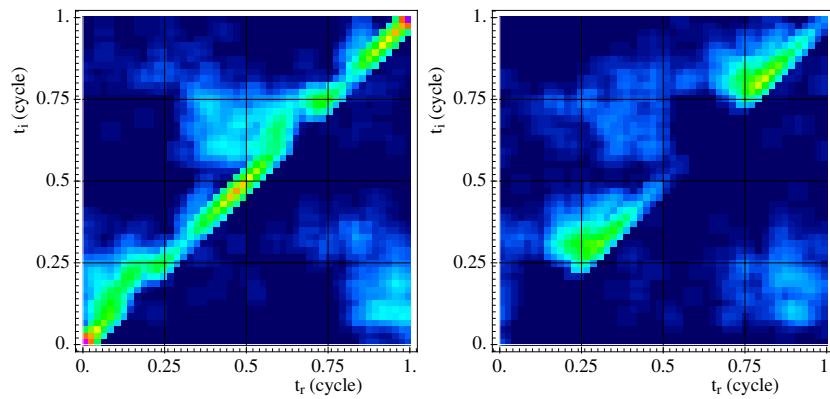


Figure 5. Phase plots for $\lambda = 1314 \text{ nm}$, $I = 5 \times 10^{14} \text{ W cm}^{-2}$. Same-side trajectories are included on left, opposite-side on right. The right-hand plot indicates that recollision ionization shortly after the field maxima can lead to opposite-hemisphere electrons. Scaling factor is 325:1.

is considerable population along the diagonal, indicating increased importance of impact ionization at recollision. We have determined the median time delay from recollision to final ionization to be 0.06 cycles, so about half the DI can be attributed to recollision impact ionization. The plot indicates more ionizations occurring near $t = 0$ or 1 c than at $t = 0.5 \text{ c}$. This is because the first ionization occurs more easily at this reduced laser frequency, and more recollisions occur in one direction than the other. Atoms which have first ionization just after 1.25 c recollide in the positive direction at approximately $t = 2 \text{ c}$. The two electrons can then be pushed into the

negative direction by the laser. This explains also the left-right asymmetry visible in figure 4.

The right-hand plot of figure 5 reveals that recollisions that occur shortly after the field maxima (0.25 and 0.75 c) can lead to significant numbers of opposite-hemisphere electrons. Because of these oppositely directed electrons the net momentum spectrum is a triplet, as shown in the centre plot of figure 4. The existence of the triplet for even a short time delay indicates that the triplet is not the result of RESI. Nonetheless, it does arise from opposite-hemisphere electrons.

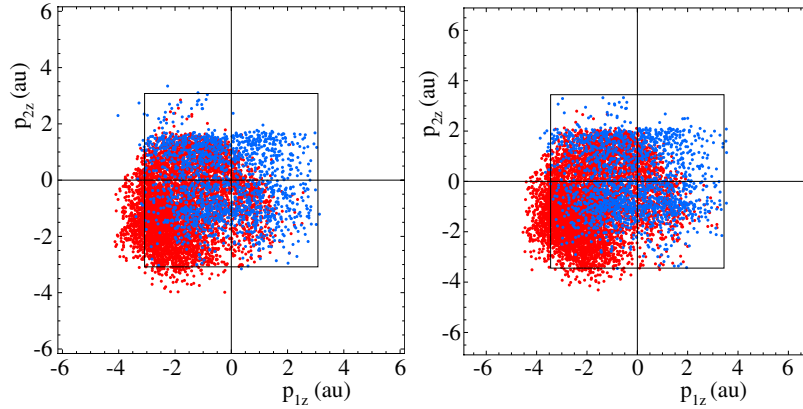


Figure 6. Scatterplot for $\lambda = 1314$ nm and two intensities 4 and 5×10^{14} W cm $^{-2}$, with the forward direction defined as positive. Trajectories are distinguished red versus blue based on whether time delay is less than or greater than 0.25 cycle, respectively. Blue is overtop of red. There are sharp cutoffs for forward propagation. Boxes indicate momentum $2\sqrt{U_p}$.

In figure 6, we show scatterplots of final longitudinal momentum p_z for intensities 4 and 5×10^{14} W cm $^{-2}$ and for the recolliding electron (vertical axis) versus the struck electron (horizontal axis). For each DI pair, the forward direction is defined as positive. Red dots indicate trajectories with time delay (from recollision to final ionization) up to 0.25 cycle, and blue dots the trajectories with longer time delay. The blue dots are shown overtop of the red. The top-left quadrant includes trajectories in which the recolliding electron continues in the forward direction but the struck electron drifts into the backward direction, either through boomeranging or pushback by the laser. As in figure 1, there is also a clear cutoff for the final momentum of the forward-drifting electron. As for $\lambda = 800$ nm, we interpret the forwardly directed electrons in terms of recollision–excitation trajectories in which the recolliding electron has sufficient energy after the collision to drift into the forward direction. Because it must deliver enough energy for the other electron to escape at a subsequent field maximum, there is a sharp energy cutoff. The blue dots in figure 6 extend further into the first quadrant than the red, and indicate having the collisionally excited electron follow the other electron into the forward direction. The second electron may have momentum up to $2\sqrt{U_p}$, indicated by the boxes.

5. The forward drift

We consider here conditions under which recollision can immediately result in a free electron that drifts into the forward direction. We employ the standard three steps model of (1) initial ionization (laser phase ωt_0 between $\pi/2$ and π), (2) acceleration by the laser field with other forces ignored, and (3) recollision (laser phase ωt_r between π and $5\pi/2$). The initial ionization time determines the energy E_r that the recolliding electron has just before recollision. Earlier initial ionizations correspond with later returns.

We treat the recollision as instantaneous, so the electron speed after recollision is

$$v_\phi = [2(E_r - \Delta E)]^{1/2}, \quad (2)$$

where ΔE denotes the energy that the electron gives up in the recollision and $\phi = \omega t_r$ indicates the laser phase the

instant after recollision⁶. If the motion is longitudinal (i.e., parallel to the laser polarization axis), the drift velocity can be approximated (neglecting forces other than from the laser) as

$$v_d = v_\phi - 2\sqrt{U_p} \cos \phi, \quad (3)$$

where the forward direction is taken as positive. Thus, for example, if recollision at the time of a laser zero ($\phi = 2\pi$) were to result in an electron at rest immediately after the collision ($v_\phi = 0$), that electron would obtain drift velocity $-2\sqrt{U_p}$, with the minus sign indicating drift into the backward direction. To examine the conditions under which v_d can be positive, we consider the limiting case in which the recolliding electron only gives up enough energy that the other electron will be able to escape over the barrier at a subsequent field maximum. For nuclear potential $-2/r$, the threshold energy for over-the-barrier escape is $-4\sqrt{\omega}U_p^{1/4}$. Thus, if the inner electron begins in the ionic ground state with energy E_g , the energy delivered must be at least

$$\Delta E_{\min} = -4\sqrt{\omega}U_p^{1/4} - E_g. \quad (4)$$

Using this minimum energy in equation (2) for v_ϕ allows us to determine numerically the maximum final drift velocity as a function of initial ionization time t_0 , laser frequency ω and ponderomotive energy U_p . All three parameters are needed. Also, any transverse velocity would imply decreased forward velocity v_ϕ immediately after the collision.

In figure 7 we plot maximum forward drift velocities for $E_g = -2$, $\lambda = 1314$ nm, and intensities $3, 4, 5$ and 6×10^{14} W cm $^{-2}$. On the left, we plot maximum forward drift velocity versus laser phase (ωt_0) at initial ionization. On the right, we divide the velocities by $\sqrt{U_p}$ and plot versus ϕ , the laser phase at recollision. The dashed curves indicate the laser field (drawn at arbitrary amplitude), and the topmost curve in the right-hand plot shows the returning electron's velocity ($/\sqrt{U_p}$) just before the collision. The sharp cutoffs that the curves in the left plot show for larger ωt_0 and, equivalently, that the curves in the right plot show for smaller ϕ are present because later initial emissions lead to earlier, less energetic

⁶ Due to electron exchange, v_ϕ may be the speed of either electron after the collision.

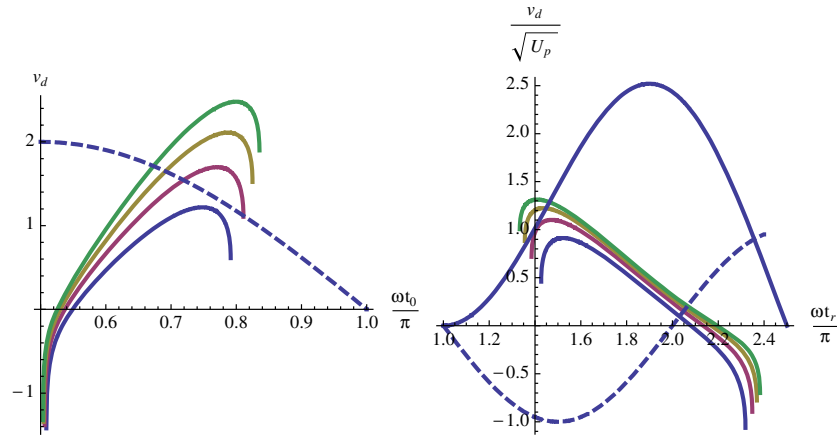


Figure 7. Calculated drift velocities for $\lambda = 1314$ nm for intensities (from bottom to top) $I = 3, 4, 5$ and 6×10^{14} W cm $^{-2}$. Left: velocities v_d versus laser phase of first electron (initial) ionization. Right: $v_d / \sqrt{U_p}$ versus phase at recollision. Dashed curves show laser field in arbitrary units, and the solid, topmost curve on the right shows electron velocity $v_d / \sqrt{U_p}$ immediately before the collision. Laser phases are expressed as multiples of π . Values of U_p are 1.78, 2.38, 2.97 and 3.56.

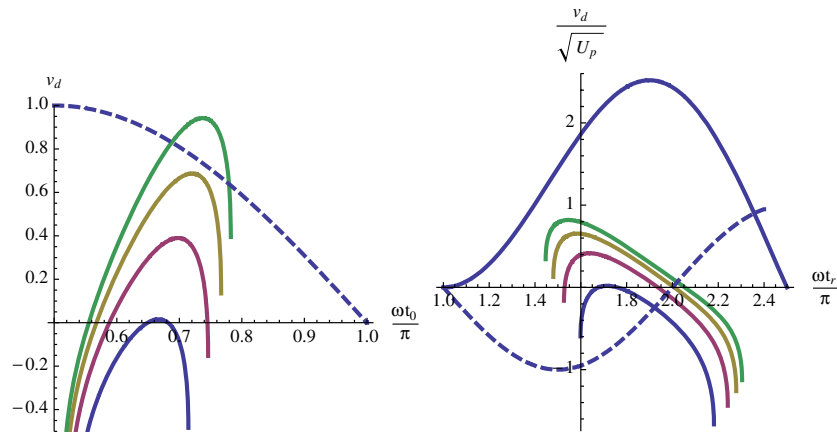


Figure 8. Electron drift velocities, repeating figure 7, but for laser wavelength 800 nm. Values of U_p are 0.66, 0.88, 1.10 and 1.32.

returns, and the return energies become too small to excite the other electron to the threshold for subsequent escape. However, earlier recollision times allow for increased forward acceleration by the laser field after the recollision. Hence, the greatest forward drift velocities do not come from the most energetic recollisions, but from collisions closer in time to the laser maximum. This result is consistent with what we saw in figure 5. The maximum values for v_d that we calculate for $I = 0.5$ PW cm $^{-2}$ closely match the ensemble cutoff velocities shown in figure 6.

Figure 8 repeats figure 7 in showing maximum drift velocities, but for $\lambda = 800$ nm. The threshold for being able to obtain a forward directed electron at recollision is reached at about $I = 3.0 \times 10^{14}$ W cm $^{-2}$.

If the recollision leaves the other electron bound, that electron may boomerang, thus giving opposite-hemisphere electrons as in quadrant two of the rightmost plot of figure 1. Delayed escape by the other electron could lead to its drifting in either direction, which explains the spillover into quadrant one of figure 1.

Rather than considering the threshold for recollision excitation, we can consider the threshold for direct ionization of the second electron. Then the minimum energy that must be delivered is simply $\Delta E_{\min} = -E_g$, which gives $v_\phi = [2(E_r + E_g)]^{1/2}$. It is straightforward to show numerically that forward drift velocity can be obtained if $U_p > 0.57|E_g|$, independent of ω . At $U_p = 0.57|E_g|$ an initial ionization that occurs at $\omega t_0 = 0.67\pi$ or 120° (0.33 cycle) leads to recollision at $\phi = \omega t_r = 1.72\pi$ or 309° (0.86 cycle) and an electron with forward velocity $v_\phi = 2\sqrt{U_p} \cos(\phi)$ just after the collision, hence zero drift velocity. The other electron would have zero velocity immediately after the collision and be pushed into the backward direction by the laser. As U_p increases above the threshold value, the range of original emissions that can lead to a forward drifting electron increases.

As U_p increases above the threshold, progressively more energy becomes available for the two electrons after recollision. The next threshold occurs when both electrons can have sufficient forward velocity after collision to drift into the forward direction. For this to occur both electrons need forward velocity v_ϕ exceeding $2\sqrt{U_p} \cos(\phi)$ just after

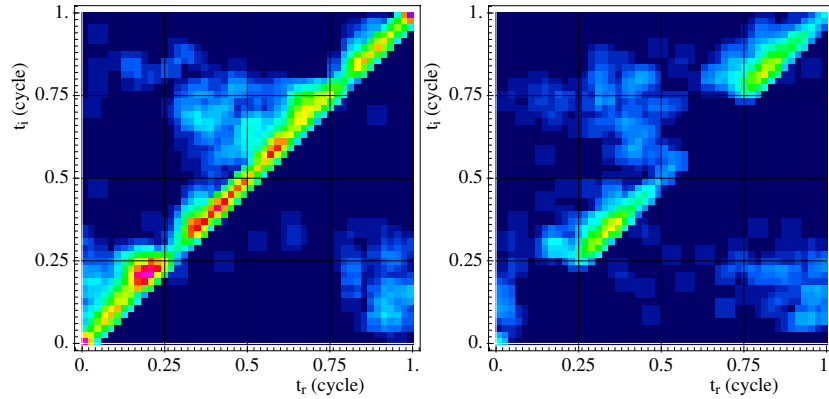


Figure 9. Phase plots for $\lambda = 2017$ nm, $I = 5 \times 10^{14}$ W cm $^{-2}$, for a 5 cycle (1+3+1) pulse. Same-hemisphere trajectories are included on the left and opposite-hemisphere trajectories on the right. Scaling factor is 125:1.

the collision. It is straightforward to show that this can occur if $U_p > 0.77|E_g|$. At the threshold for having two forward drifting electrons, the return time is 0.80 cycles or 1.60π (287°) and original emission time is 0.36 c or 0.715π (129°). Of course, near the threshold value the two electrons would need to share energy nearly equally for both to drift into the forward direction. Unequal sharing would lead to electrons drifting out in opposite directions, just as we found in figure 5 for $\lambda = 1314$ nm. Our experience has been that equal energy sharing is very unusual; hence, we would expect that the system would need to be well above threshold before forward travelling pairs became common.

6. Laser wavelength 2017 nm

Figure 9 shows final ionization phase versus recollision phase for wavelength 2017 nm and for the same intensity of 5×10^{14} W cm $^{-2}$. It shows that recollision ionizations occur over a wide range of laser phases, including just before laser maxima (0.25 and 0.75 c). Having recollision ionization occur before the laser maximum assures forward drift. Mathematically, we would have $\cos\phi < 0$ in equation (3). We can also obtain forward–forward pairs from other collision times, since we are above the threshold determined in the previous paragraph. One can expect some variation in relative electron energies immediately after impact DI, with lower energy electrons pushed into the backward direction. Thus, we obtain opposite-hemisphere electrons, as indicated in the right-hand plot, as well as same-hemisphere electrons.

The net longitudinal momentum spectrum is displayed in the rightmost plot of figure 4. It is again a doublet, but with a central region from the opposite-hemisphere electrons.

As an aside, we note that we have smaller DI yield at this large wavelength. The barrier is suppressed for much longer each half cycle. Consequently, more first ionizations occur before the field maximum and a smaller fraction of electrons return for recollision. We note also that for our laser parameters the oscillation amplitude for a free electron E_0/ω^2 evaluates to 234 au (99 au for $\lambda = 1314$). A sufficiently large laser focus would be needed, or else one might need to take into account changes in laser intensity with position.

7. Conclusions

We have examined how NSDI within classical models varies with laser wavelength. Changing the wavelength but not intensity changes the ponderomotive energy U_p , and thus the energy at recollision. When the wavelength is increased in our model the net or sum longitudinal momentum transitions from a singlet at wavelength 483 nm to a doublet at 800 nm, then a triplet at 1314 nm, then back to a doublet at 2017 nm. The short wavelength case has been examined elsewhere [18], where we discussed how recollision excitation could lead to a doubly excited state that would decay into oppositely travelling electrons. At 780 or 800 nm, the most common scenario for NSDI is recollision excitation. One electron remains free after the recollision and is swept into the backward direction by the laser. The other electron is bound but often boomerangs [9] (is pulled back by the nucleus) and escapes into the backward direction at the first laser maximum after the recollision. However, already at 3×10^{14} W cm $^{-2}$ we are well above the threshold for one electron to be able to retain enough energy at recollision excitation that it can overcome the backward push from the laser field and drift into the forward direction. Such electrons are a small part of the total at 800 nm, but become much more important at 1314 nm. Because the other electron is likely to be pushed back by the laser field, oppositely directed electrons can be obtained, giving rise to a central peak in the spectrum. At this long wavelength, the outer peaks are well separated and the central peak distinct, so the spectrum becomes a triplet. At still higher wavelengths we cross the threshold for having two forward directed electrons after recollision impact ionization. That suppresses the centre peak, so that the spectrum is again a doublet.

Recent experiments by Rudenko *et al* [5] have looked at variation of the momentum spectrum with laser intensity. They have seen how the doublet collapses to a singlet as systems transition from NSDI to sequential ionization. It may be that in the transitional region, the growing central spike is not just from sequential ionization, but from recollision generated forward–backward (or ‘Z’) combinations [4] such

as we have discussed here. We expect that in order to see these combinations unambiguously, longer wavelengths would be needed.

In their experiments, Alnaser *et al* [17] have seen the transition from doublet to singlet in the spectrum for Ne^{2+} for increasing intensity at wavelength 1314 nm, but with no triplet. We are continuing to investigate the species dependence of the effects we have been considering. Forward travelling electrons can be produced from recollisions that occur while the laser field is strong, but such recollisions occur in the three-step model only if first ionizations can occur fairly late in a laser pulse. It may be that it is too difficult to ionize the first electron from neon (which has high binding energy) for the triplet to be seen there.

Acknowledgments

This material is based upon work supported by Calvin College and by the National Science Foundation under grant No. 0653526 to Calvin College. We acknowledge also our ongoing collaboration with J H Eberly's group at the University of Rochester.

References

- [1] For reviews, see Dörner R *et al* 2002 *Adv. At. Mol. Opt. Phys.* **48** 1–34
Ullrich J *et al* 2003 *Rep. Prog. Phys.* **66** 1463–545
Becker A, Dörner R and Moshhammer R 2005 *J. Phys. B: At. Mol. Opt. Phys.* **38** S753–72
- [2] See, for example, Weber Th *et al* 2000 *Phys. Rev. Lett.* **84** 443–6
Moshhammer R *et al* 2000 *Phys. Rev. Lett.* **84** 447–50
- [3] Chen J and Nam C H 2002 *Phys. Rev. A* **66** 053415
- [4] Ho P J and Eberly J H 2003 *Opt. Express* **11** 2826–31
Ho P J, Panfili R, Haan S L and Eberly J H 2005 *Phys. Rev. Lett.* **94** 093002
- [5] Rudenko A *et al* 2008 *Phys. Rev. A* **78** 015403
- [6] Corkum P B 1993 *Phys. Rev. Lett.* **71** 1994–7
Schafer K J, Yang B, DiMauro L F and Kulander K C 1993 *Phys. Rev. Lett.* **70** 1599–602
- [7] Becker A and Faisal F H M 2000 *Phys. Rev. Lett.* **84** 3546
Chen J, Liu J, Fu L B and Zheng W M 2000 *Phys. Rev. A* **63** 011404
- [8] Haan S L, Breen L, Karim A and Eberly J H 2006 *Phys. Rev. Lett.* **97** 103008
Haan S L, Breen L, Karim A and Eberly J H 2007 *Opt. Express* **15** 767
- [9] Haan S L and Smith Z S 2007 *Phys. Rev. A* **76** 053412
- [10] Haan S L, Smith Z S and VanDyke J S 2008 *Phys. Rev. Lett.* **101** 113001
- [11] Rudenko A *et al* 2004 *Phys. Rev. Lett.* **93** 253001
- [12] Feuerstein B, Moshhammer R and Ullrich J 2000 *J. Phys. B: At. Mol. Opt. Phys.* **33** L823–30
Kopold R, Becker W, Rottke H and Sandner W 2000 *Phys. Rev. Lett.* **85** 3781
- [13] Witzel B, Papadogiannis N A and Charalambidis D 2000 *Phys. Rev. Lett.* **85** 2268
- [14] Parker J S, Doherty B J S, Taylor K T, Schultz K D, Blaga C I and DiMauro L F 2006 *Phys. Rev. Lett.* **96** 133001
- [15] Staudte A *et al* 2007 *Phys. Rev. Lett.* **99** 263002
Rudenko A *et al* 2007 *Phys. Rev. Lett.* **99** 263003
- [16] Emmanouilidou A 2008 *Phys. Rev. A* **78** 023411
Ye D F, Liu X and Liu J 2008 *Phys. Rev. Lett.* **101** 233003
- [17] Alnaser A S *et al* 2008 *J. Phys. B: At. Mol. Opt. Phys.* **41** 031001
- [18] Haan S L, Smith Z S, Shomsky K N and Plantinga P W 2008 *J. Phys. B: At. Mol. Opt. Phys.* **41** 211002
- [19] Grobe R and Fedorov M V 1992 *Phys. Rev. Lett.* **68** 2592
- [20] Panfili R, Haan S L and Eberly J H 2002 *Phys. Rev. Lett.* **89** 113001